
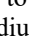
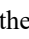

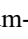


Empirical Analysis of the Impact of Additional Padding on the Collaborative Robot Velocity Behavior in Transient Contact Cases

Christopher Schneider¹^a, Maximilian M. Seizmeir¹^b, Thomas Suchanek¹^c,
Martina Hutter-Mironovová¹^d, Mohamad Bdiwi²^e and Matthias Putz²
¹*Department of Product Management and Safety, Yaskawa Europe GmbH, Allershausen, Germany*
²*Fraunhofer IWU Machine Tools and Forming Technology, Chemnitz, Germany*

Keywords: Biomechanical Thresholds, Collaborative Robots, Force and Pressure Measurements, Machine Tending, Transient Contact.


Abstract: In this paper, a suitable measurement setup is presented and applied to conduct force and pressure measurements for transient contact cases with the shoulder at the example of lathe machine tending. Empirical measurements were executed on a selected collaborative robot's behavior regarding allowable operating speeds under consideration of sensor sensitivity, robot collision geometry, and damping materials. Comparisons between the theoretic calculations proposed in ISO/TS 15066 and the practical measurement results present a basis for future research. With the created database, preliminary risk assessment and economic assessment procedures of collaborative machine tending cells can be facilitated.


1 INTRODUCTION


Within the last years, collaborative robot (cobot) machine tending installations increased rapidly with growing potential to become one of the main cobot applications (BIS Research 2016). Due to their high usability and fenceless operation, systems can be adapted to new requirements conveniently. Small- and medium-sized companies (SME's) with high-mix-low-volume production programs increasingly benefit from the flexibility enhancements of robotic machine loading and unloading. However, end-users are confronted with an extensive risk assessment when it comes to safety and CE marking, especially regarding the force and pressure measurements defined in ISO/TS 15066:2016 (Fraunhofer Institute for Industrial Engineering IAO 2016). To prevent injuries, the application must comply with body-region-specific biomechanical threshold values that determine the allowed velocity the robot can operate at and, therefore, the achieved cycle time (DGUV


2017). Since these tests must be executed on-site, a prototypical cell is required, usually available at a well-advanced planning stage of an automation project. Economic considerations, on the other side, are required already at the project's beginning to determine a return on investment (ROI) upfront. On this basis, the investment can be justified regarding other automation options, such as linear axis or fenceless industrial robots. Since the achieved collaborative operating speeds are determined at the end of the project, investment reliability and trust in the automation solution are inhibited.


Currently, the dominant guideline is the ISO/TS 15066, which provides equations to calculate the allowed collaborative speeds for a collision in free space (transient contact). As an option, the compliant velocities can also be determined by practical tests. Despite the progress made in human-robot collaboration during the last years, influencing factors on the velocity results, system parameter modeling, and demonstrated risk assessment procedures are

^a  <https://orcid.org/0000-0003-2903-8347>

^b  <https://orcid.org/0000-0002-5755-4405>

^c  <https://orcid.org/0000-0002-8366-3066>

^d  <https://orcid.org/0000-0001-5823-8159>

^e  <https://orcid.org/0000-0001-7070-9988>

lacking, leading to mismatching with the needs of end-users.

This paper aims to reveal insights on the maximum allowed collaborative speed (MACS) for a selected robot model. Other cobot models are welcomed to replicate the proposed test setup to provide comparison values and contribute to a mutual empirical database. In the future, such databases can help to facilitate the risk and economic assessment procedure. In the presented empirical study, different typical transient contact cases in lathe machine trending have been analyzed regarding the influence of sensor sensitivity settings and additional padding on the force and pressure development. Comparisons to the equations provided by the technical specification show potential future research fields. This paper contributes to fundamental research regarding robot behavior modeling in transient contact cases, emphasizing biomechanical threshold values.

2 THEORY

A general overview of different aspects of safety is given by Chemweno et al. (2020), Lasota et al. (2014), Marvel and Bostelman (2014), Robla-Gómez et al. (2017), and Villani et al. (2018). As defined in ISO/TS 15066:2016, two contact situations in human-robot collaboration have been distinguished. Quasi-static or clamping contacts occur when continuously increasing weight is partially compensated by elastic deformation. Transient cases or collisions in free space, on the other side, force the collision object to move in the resultant impact direction. Human subject research empirically derived biomechanical threshold values for forces and pressures to avoid operator injuries, depending on the respective body region. These values serve as a database for the risk assessment of collaborative work cells and have been adopted by ISO/TS 15066 (2016). Several studies by Behrens and Pliske (2019) gave indications for further refining and expansion of these thresholds. To execute such a risk assessment, the whole system (robot, gripper, workpiece) must be analysed regarding potential collision situations, based on the programmed paths, work environment and possible human behaviour. For the identified cases, forces and pressures are measured with designated devices, that are available from different manufacturers. Problematic in this procedure is the requirement of a prototypical cell for the measurements, which requires already a high-quality concept of the planned system. Such measurement

devices have a load cell integrated, that measures the force development over time to generate a time-dependent force graph with a respective software. Pressures are measured with sensitive foils, that are placed on top of the device. Small air bubbles burst during the collision event, discolouring the film dependent on the intensity. By scanning each foil, the results can be digitized for visualization and further analysis. Additionally, to the device itself, exchangeable damping materials (K1) and springs supplement the simulation of body parts by their combination of material characteristics and spring constants.

As mentioned earlier, this procedure is situation-individual and therefore difficult to generalize, especially regarding the upfront determination of compliant robot operating speeds. This leads to a static risk consideration that is specific for a designated case without adaption capabilities. Operation in dynamic environments (i.e., deviating workpieces), as described in Eder et al. (2014), would require a permanent re-evaluation of the risk assessment. Such safety-adaptive systems would need a solid classification of risk cases as well as a thorough robot behavior modeling. In the current research, different approaches analyze quasi-static and transient contact cases, presented as follows.

To characterize collisions, Haddadin et al. (2017) presented a multi-phase procedure with the classification criteria force's direction and intensity as well as occurrence, severity, and duration. Vemula et al. (2018) introduce the power flux density as a metric under consideration of energy transfer and contact duration. Furthermore, a rapid contact model is presented and tested. Svarny et al. (2020) developed a collision force map that is three-dimensionally dependent on the robot's operating space. Empirical measurements with the cobots UR10e and KUKA LBR Iiwa analyze the impact of robot pose, distance, and velocity. Several crash tests with different industrial robots have been executed by Haddadin et al. (2011), emphasizing robot mass and velocity and singularity forces during clamping. Further crash tests were conducted by Weitschat (2019) under the use of a robotic airbag protecting the workpiece to analyze its effect on the resulting forces and pressures. Force calculation models for quasi-static cases were published by Ganglbauer et al. (2020) and Kovincic et al. (2019). Virtual force sensors and simulations were presented in Shin et al. (2019) and Yen et al. (2019).

3 MATERIALS AND METHODS

3.1 Risk Assessment and Experimental Setup

A preliminary risk assessment of lathe machine tending applications identified multiple transient contacts based on typical movement sequence simulations. For both the feed motion (insert and take out the workpiece) and the movement between door and feed position, the cobot can collide with the operator at the marked areas, illustrated in Figure 1. The transparent position represents the start point, while the opaque one shows the target coordinate. Assuming a robot installation on a 900mm high pedestal, the motions will likely be executed at the operator's shoulder height. Therefore, this body part is emphasized in this paper.

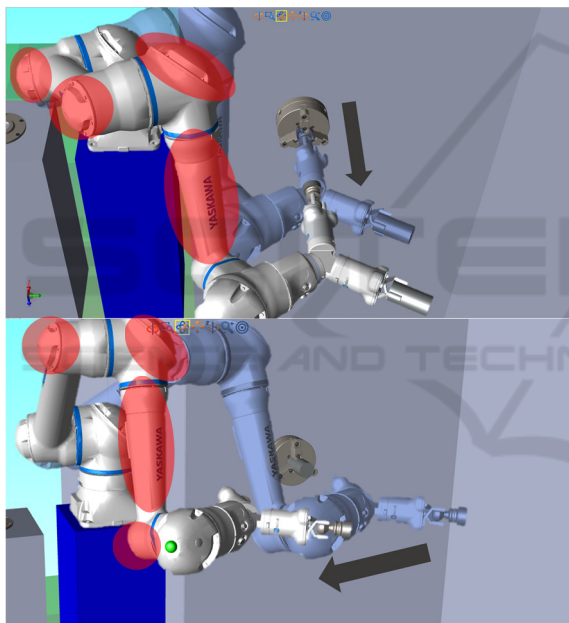


Figure 1: Potential Transient Risk Areas.

A Yaskawa HC10DT IP67 cobot installed on a 900mm high pedestal bolted to the ground was used for the experiments. To replicate the identified values, the software version YAS4.12.01A(EN/DE)-00 can be used. For realistic reproduction of the transient collision case, a special design guarantees free oscillation and is adjustable in weight to match the shoulder mass properties of $m=40\text{kg}$. Therefore, a large locating bolt with a thread was used to install different weight plates with a screw nut. This unit was connected to the steel tracks of a 0,5t crane, minimizing friction and providing a sufficiently long

pendulum. On top of the plates, the measurement device PILZ PRMS has been fixed using screw clamps. The pedestal-crane-combination has been adjusted to simulate a realistic shoulder height of 1450mm. For reproducible results, ropes were attached to the device to guide the recoil movement and maintain a certain rebound angle.

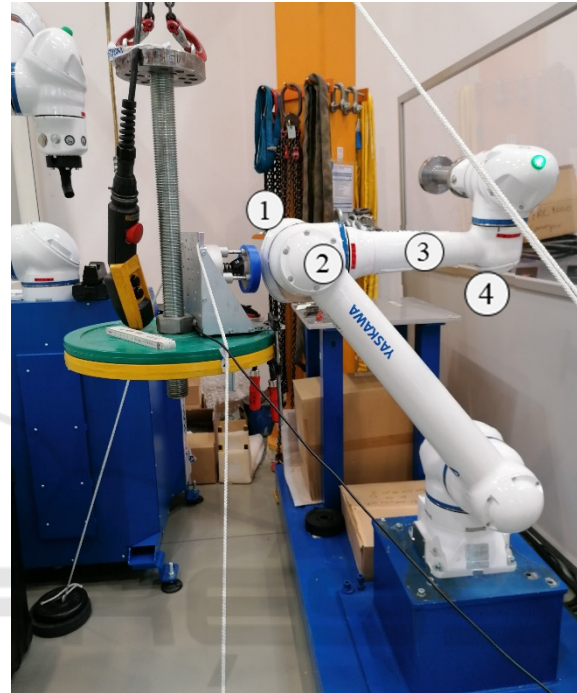


Figure 2: Measurement Setup for Shoulder Simulation with 1 Elbow Big Cap, 2 Elbow Small Cap, 3 Forearm and 4 Wrist Cap.

3.2 Considered Influencing Factors

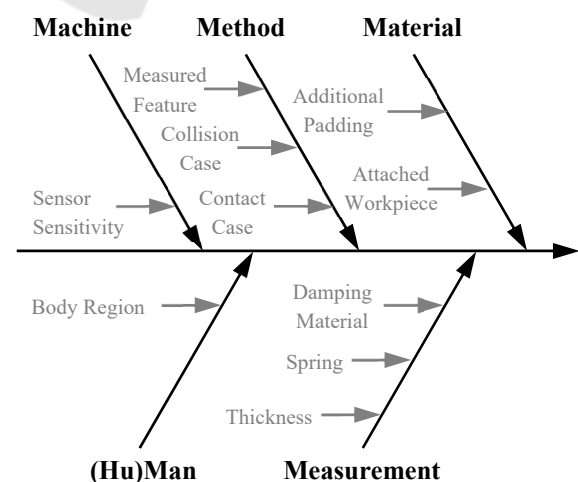


Figure 3: Ishikawa Diagram with Influencing Factors on the Maximum Allowed Collaborative Speed.

To collect possible influencing factors on the maximum allowed collaborative speed (MACS), an Ishikawa diagram has been created based on the 5M's machine, method, material, (hu)man, and measurements. For further specification, detailed characteristics have been assigned that are used as a basis for experiment planning and design.

Table 1: Influencing Factors on the Maximum Allowed Collaborative Speed.

5 M's	Criteria	Characteristics
Machine (Robot)	Robot Collision Geometry	Elbow Big Cap, Elbow Small Cap, Forearm, Wrist Cap
	Sensor Sensitivity	50N, 100N
	Software Version	YAS4.12.01A(EN/DE)-00
Method	Measured Feature	Individual
	Collision Case	Transient
(Hu)man	Body Region	Shoulder
	Force Threshold	420N
	Pressure Threshold	320N/cm ²
Measurement	Damping Material K1	Shore A 30
	Spring K2	35N/mm
	Thickness	14mm
Material	Padding	None, Neoprene, Foam

3.3 Experimental Design

To cover the predefined risk cases, four different robot outer contours have been tested regarding collision forces and pressures: the two elbow caps, the forearm, and the wrist cap of the cobot (see Figure 2). This setup was designed to deliver insights on worst-case scenarios where one of the robot's least favorable edges collides with the measurement device. While the hard edge has been used for tests with the big elbow cap, this type of collision was not reproducible for the smaller caps since the cap radius does not allow a collision with the cap edge. Instead, contacts with the round outer contour of the small caps were targeted. Therefore, the big elbow cap delivers a smaller contact area than the small caps. As can be seen in Figure 1, different movement types are assigned to the respective contact areas. While tests with the big elbow cap utilize mainly the 2nd robot axis for linear movement execution, the other cases predominantly use the 1st axis.

Furthermore, measurements have been conducted with different protective measures on the collision surface: no protection, neoprene padding (thickness: 5mm), and foam padding (expanded polyethylene foam profile, thickness: 140mm, see Figure 4.). While the neoprene protection was attached with a velcro fastener, the foam protection had to be attached with adhesive tape. Using these three different paddings, the impact of the damping characteristics regarding material and thickness on the MACS is analyzed.

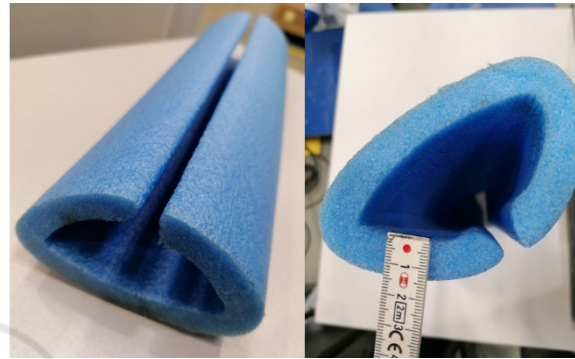


Figure 4: EPE Foam Profile.

According to DGUV (2017) and ISO/TS 15066 (2016), a spring constant of $k=35\text{N/mm}$, blue silicone damping material with shore A 30 hardness, and a thickness of 14mm must be used for the measurement device to match the shoulder.

According to the PRMS manual, three force measurements per series are recommended to counterbalance the device's inaccuracies. To provide scientific and statistically valid results, ten measurements run have been performed. From these data, the maximal and minimal values each have been considered as outliers and therefore excluded. Based on the eight remaining values, the average has been calculated, which serves as a comparison basis with the threshold values. The documented average environment conditions of 60% humidity and 21°C temperature lie within the stated tolerance of 35%-80% and 17°C to 35°C. Following the manual, 30 minutes waiting time between pressure foil measurement and scanning has been adhered to.

For worst-case scenario consideration, a workpiece with maximum payload utilization was used. Therefore, a steel shaft with 110mm in diameter, 230mm in length, and 6,041kg weight was manufactured and attached.

To determine the MACS, iterative velocity adjustment loops with a predefined scaling of 10mm/s led finally to one threshold-compliant and one violating speed, while the last conform one is the MACS. For valid results, the distance between the

programmed start and endpoint must be sufficiently high to guarantee that the robot reaches its predefined velocity. Furthermore, the second coordinate must lie at a fair distance behind the collision point to avoid decelerating the robot before impact. Correct configured tool data and regularly calibrated torque sensors ensure consistent measurement quality. As robot-dependent factors, different sensor sensitivity settings, adjustable in the safety controller with force limits in N, were used. For this research, 100N and 50N were considered.

4 RESULTS

4.1 Theoretical Considerations

Firstly, the MACS will be determined by applying the respective equations defined in ISO/TS 15066. Table 2 shows the relevant factors and obtained input data for the human shoulder joint as well as the selected robot contact areas.

Table 2: Factors for Transient Velocity Calculations.

Factor	Symbol	Value	Unit
Transfer Energy	E	2,5	$\frac{kg \cdot m^2}{s^2}$
Maximum Contact Force	F_{max}	420	N
Maximum Contact Pressure	p_{max}	3.200.000	$\frac{N}{m^2}$
Effective Spring Constant	k	35.000	$\frac{N}{m}$
Contact Area Elbow	A_{Elb}	$1,05 * 10^{-4}$	m^2
Contact Area Arm	A_{Arm}	$1,6 * 10^{-3}$	m^2
Contact Area Cap	A_{Cap}	$9,621 * 10^{-4}$	m^2
Relative Speed	v_{rel}	calculated	$\frac{m}{s}$
Allowed Speed Robot Elbow	v_{Elb}	calculated	$\frac{m}{s}$
Allowed Speed Robot Arm	v_{Arm}	calculated	$\frac{m}{s}$
Allowed Speed Robot Cap	v_{Cap}	calculated	$\frac{m}{s}$
Reduced Mass	μ	calculated	kg
Effective Mass of the Human Body Region	m_H	40	kg
Effective Mass of the Robot	m_R	calculated	kg
Effective Payload of the Robot System	m_L	6,041	kg
Total Mass of Moving Robot Parts	M	58	kg

Based on this information, the MACS of the transient contact case is calculated based on energy, maximum permissible force, and maximum permissible pressure. These results will be compared and discussed with experimentally measured values.

Preliminary Calculations:

$$m_R = \frac{M}{2} + m_L = 35,041kg \quad (1)$$

$$\mu = \left(\frac{1}{m_H} + \frac{1}{m_R} \right)^{-1} = 18,678kg \quad (2)$$

Calculations based on Energy:

$$E = \frac{1}{2} \mu v_{rel}^2 \quad (3)$$

$$v_{rel} = \sqrt{\frac{2E}{\mu}} = 0,517 \frac{m}{s} \quad (4)$$

Calculations based on Permissible Force:

$$v_{rel} = \frac{F_{max}}{\sqrt{\mu k}} = 0,519 \frac{m}{s} \quad (5)$$

Calculations based on Permissible Pressure:

$$v_{Elb} = \frac{p_{max} \cdot A_{Elb}}{\sqrt{\mu k}} = 0,415 \frac{m}{s} \quad (6)$$

$$v_{Arm} = \frac{p_{max} \cdot A_{Arm}}{\sqrt{\mu k}} = 6,332 \frac{m}{s} \quad (7)$$

$$v_{Cap} = \frac{p_{max} \cdot A_{Cap}}{\sqrt{\mu k}} = 3,808 \frac{m}{s} \quad (8)$$

While the energy- and force-based calculations lead to nearly similar results, the pressure-based calculations deviate with a factor between 0,8 and 12,3. Consequently, the forces and energies are the theoretical limiting factors, while pressure could be strongly increased according to the calculated results.

4.2 Experiment on Elbow Big Cap

Without protective measures, the maximum speed is mainly restricted by the pressure limit, which has been surpassed at 70mm/s, leading to a MACS of 60mm/s. However, with protective measures, the MACS climbs up to 720mm/s with neoprene and 770mm/s with foam padding. This can be explained by an even pressure distribution on a greater surface compared to measurements without protection. Furthermore, the MACS with a force limit of 50N was slightly higher than measurements with 100N for protective measures while having no effect when using no padding.

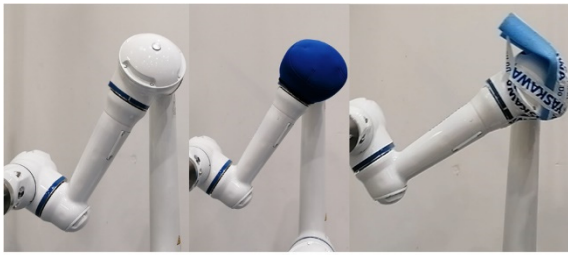


Figure 5: Setup for Elbow Big Cap.

4.3 Experiment on Elbow Small Cap

The pressure threshold has not been reached in this experiment for all three setups, while the force has been exceeded at 890mm/s to 920mm/s depending on the used padding. Measurement results with 50N deliver higher MACS compared to the 100N force limit, irrespective of the protective measures. No clear tendency on the dependency of MACS and the protective measure could be identified.



Figure 6: Setup for Elbow Small Cap.

4.4 Experiment on Forearm

Pressure thresholds were undercut with all measurement series. The highest MACS have been registered for 100N force limit and measurement without protection at 750mm/s. With a force limit of 50N, the MACS could not be reached for neoprene and foam protection since the high torque sensor sensitivity triggers a protective stop of the robot during high acceleration.

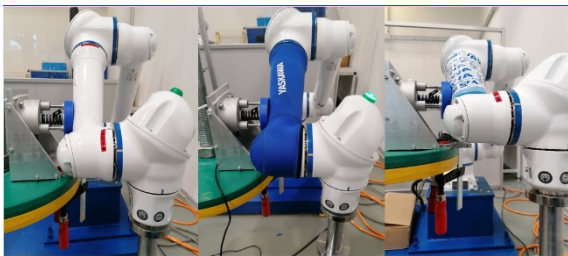


Figure 7: Setup for Forearm.

4.5 Experiment on Wrist Cap

As expected, observed MACS are lower than those of the small elbow cap because the collision point is further away from the robot base resulting in a higher lever. The highest MACS was registered for the 50N force limit in combination with foam protection. Without protection, results were lower for both sensor sensitivities.

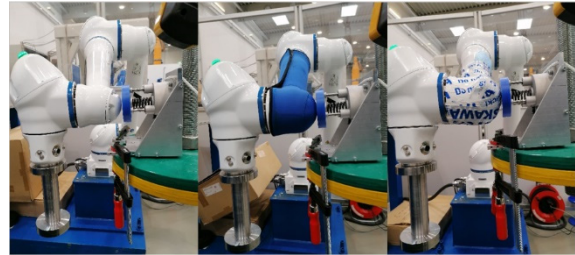


Figure 8: Setup for Wrist Cap.

4.6 Summary

Additional padding on the respective collision surface can drastically increase the maximum allowed collaborative speed, if critical areas with small surfaces (big elbow cap) are present. For the other three cases, a clear influence of protective measures on the MACS could not be verified. Whereas the neoprene cover could not evidently reduce occurring force compared to the setup without protection, attaching EPE foam profiles on the collision surface showed significant force reduction. Overall, the pressure threshold has been exceeded only for the big elbow cap without padding.

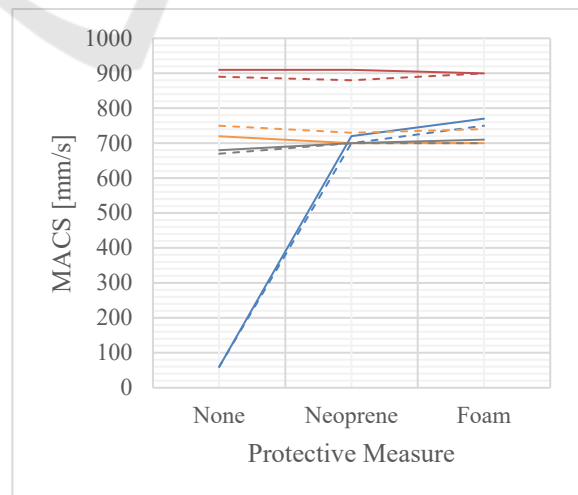


Figure 9: MACS by Protective Measures and Force Limit: 50N – Full, 100N – Dotted, Elbow Big Cap – Blue, Elbow Small Cap – Red, Forearm – Green, Wrist Cap – Black.

5 CONCLUSIONS

In this paper, the influence of additional padding in transient contact cases has been analyzed. Based on the use case of lathe machine tending, different contact cases were concluded in a preliminary risk assessment, based on the required movements with the respectively affected robot geometries as an interfering contour. As a realistic body region, the shoulder was assumed to collide with the robot during either a feed motion between the machine's door and spindle feed position or between spindle feed and spindle position. To cover robot-specific influencing factors, force limits of 50N and 100N were tested. As theoretical fundament, the maximum allowed collaborative velocities were calculated with the equations defined in ISO/TS 15066. A high result deviation has been demonstrated depending on the used metric (energy, force or pressure). Comparisons to the empirically determined MACS values show differences of 0,25m/s to 0,46m/s for the big elbow cap, 0,38m/s to 2,91m/s for the elbow small cap, 0,18m/s to 5,6m/s for the forearm and 0,15m/s to 3,14m/s for the wrist cap. Due to the used test setup, measurement deviations can be traced back to the oscillation of the hanging construction during a collision and the result accuracy of the pressure-sensitive foils. The force limit settings (sensor sensitivity) showed a small impact on the result since the robot stops immediately when colliding. Experiments on the forearm with a 50N force limit were not feasible due to the robot sensors' self-triggering at high velocities.

This study was executed with a selected cobot and is therefore exclusively valid for this model. To help building a broader database of the maximum allowed collaborative speeds and to understand various influencing factors, similar tests with other cobot models are required in the future. For safety engineering, this data would serve as a tool to facilitate the risk assessment effort on-site to reduce certification time and cost. Increased precision in the upfront determination of compliant speeds improves investment reliability since cycle times can be approximated in an early project stage. Such a database supports performance transparency of different robot models regarding achievable cycle times and helps the robot planner and end-user select the most profitable cobot. Lastly, robot manufacturers gain valuable insights for further R&D activities to improve their products.

ACKNOWLEDGEMENTS

We thank Dr.-Ing. Roland Behrens (Fraunhofer IFF) for consulting throughout the project, especially regarding the measurement setup's suitability.

REFERENCES

- Behrens, R.; Pliske, G. (2019): Human-Robot Collaboration: Partial Supplementary Examination [of Pain Thresholds] for Their Suitability for Inclusion in Publications of the DGUV and Standardization. Fraunhofer IFF, Otto von Guericke University Trauma Surgery Clinic.
- BIS Research (2016): Global Collaborative Robot Hardware Market, Analysis & Forecast, 2016-2021 (Focus on Major Industries and Applications). BIS Research. Available online at <https://bisresearch.com/industry-report/global-cobots-market-report-forecast.html>, checked on 5/14/2021.
- Chemweno, P.; Pintelon, L.; Decre, W. (2020): Orienting safety assurance with outcomes of hazard analysis and risk assessment: A review of the ISO 15066 standard for collaborative robot systems. In *Safety Science* 129. DOI: 10.1016/j.ssci.2020.104832.
- DGUV (2017): Collaborative robot systems: Design of systems with "Power and Force Limiting" function. Available online at https://www.dguv.de/medien/fb-holzundmetall/publikationen-dokumente/infoblaetter/infobl_englisch/080_collaborativerobotsystems.pdf, updated on 08/2017, checked on 3/12/2021.
- Eder, K.; Harper, C.; Leonards, Z. (Eds.) (2014): Towards the Safety of Human-in-the-Loop Robotics: Challenges and Opportunities for Safety Assurance of Robotic Co-Workers. The 23rd IEEE International Symposium on Robot and Human Interactive Communication. Edinburgh, UK, 25-29 Aug. 2014: IEEE.
- Fraunhofer Institute for Industrial Engineering IAO (2016): Lightweight robots in manual assembly - best to start simply! Edited by W. Bauer, M. Bender, M. Braun, P. Rally, O. Scholtz. Available online at <https://www.produktionsmanagement.iao.fraunhofer.de/content/dam/produktionsmanagement/de/documents/LBR/Studie-Leichtbauroboter-Fraunhofer-IAO-2016-EN.pdf>, checked on 5/13/2021.
- Ganglbauer, M.; Ikeda, M.; Plasch, M.; Pichler, A. (2020): Human in the loop online estimation of robotic speed limits for safe human robot collaboration. 30th International Conference on Flexible Automation and Intelligent Manufacturing (FAIM2021). In *Procedia Manufacturing* 51, pp. 88–94. DOI: 10.1016/j.promfg.2020.10.014.
- Haddadin, S.; Albu-Schäffer, A.; Hirzinger, G. (2011): Safe Physical Human-Robot Interaction: Measurements, Analysis and New Insights. In *Robotics Research*, pp. 395–407. DOI: 10.1007/978-3-642-14743-2_33.

- Haddadin, S.; De Luca, A.; Albu-Schäffer, A. (2017): Robot Collisions: A Survey on Detection, Isolation, and Identification. In *IEEE Transactions on Robotics* 33 (6), pp. 1292–1312. DOI: 10.1109/TRO.2017.2723903.
- Kovincic, N.; Gattringer, H.; Müller, A.; Weyrer, M.; Schlotzhauer, A.; Kaiser, L.; Brandstötter, M. (2019): A model-based strategy for safety assessment of a robot arm interacting with humans. In *Proceedings in Applied Mathematics & Mechanics*. DOI: 10.1002/pamm.201900247.
- Lasota, P. A.; Fong, T.; Shah, J. A. (2014): A Survey of Methods for Safe Human-Robot Interaction. In *Foundations and Trends* 5 (4), pp. 261–349. DOI: 10.1561/9781680832792.
- Marvel, J.; Bostelman, R. (2014): A Cross-domain Survey of Metrics for Modelling and Evaluating Collisions. In *International Journal of Advanced Robotic Systems* 11. DOI: 10.5772/58846.
- Robla-Gómez, S.; Becerra, V. M.; Llata, J. R.; González-Sarabia, E.; Torre-Ferrero, C.; Pérez-Oria, J. (2017): Working Together: A Review on Safe Human-Robot Collaboration in Industrial Environments. In *IEEE Access* 5, pp. 26754–26773. DOI: 10.1109/ACCESS.2017.2773127.
- ISO/TS 15066:2016, 2016: Robots and robotic devices - Collaborative robots.
- Shin, H.; Kim, S.; Seo, K.; Rhim, S. (Eds.) (2019): A Real-Time Human-Robot Collision Safety Evaluation Method for Collaborative Robot. 3rd IEEE International Conference on Robotic Computing (IRC). Naples, Italy, 25.02.-27.02.: IEEE.
- Svarny, P.; Rozlivek, J.; Rustler, L.; Hoffmann, M. (2020): 3D Collision-Force-Map for Safe Human-Robot Collaboration (Preprint).
- Vemula, B.; Matthias, B.; Ahmad, A. (2018): A design metric for safety assessment of industrial robot design suitable for power- and force-limited collaborative operation. In *International Journal of Intelligent Robotics and Applications* 2, pp. 226–234. DOI: 10.1007/s41315-018-0055-9.
- Villani, V.; Pini, F.; Leali, F.; Secchi, C. (2018): Survey on human–robot collaboration in industrial settings: Safety, intuitive interfaces and applications. In *Mechatronics* 55, pp. 248–266. DOI: 10.1016/j.mechatronics.2018.02.009.
- Weitschat, R. (2019): Industrial Human-Robot Collaboration: Maximizing Performance While Maintaining Safety. Dissertation. Universität Rostock. Fakultät für Maschinenbau und Schiffstechnik.
- Yen, S.-H.; Tang, P.-C.; Lin, Y.C.; Lin, C.-Y. (2019): Development of a Virtual Force Sensor for a Low-Cost Collaborative Robot and Applications to Safety Control. In *Sensors* 19 (11). DOI: 10.3390/s19112603.